

*For
28 March*

NACA TN 2658

NATIONAL ADVISORY COMMITTEE FOR AERONAUTICS

TECHNICAL NOTE 2658

LAMINAR BOUNDARY LAYER OVER FLAT PLATE
IN A FLOW HAVING CIRCULAR STREAMLINES

By Artur Mager and Arthur G. Hansen

Lewis Flight Propulsion Laboratory
Cleveland, Ohio

20000731 106



Washington

March 1952

Reproduced From
Best Available Copy

DISTRIBUTION STATEMENT A
Approved for Public Release
Distribution Unlimited

DTIC QUALITY INSPECTED 4

AGMOO-10-3101

NATIONAL ADVISORY COMMITTEE FOR AERONAUTICS

TECHNICAL NOTE 2658

LAMINAR BOUNDARY LAYER OVER FLAT PLATE IN A FLOW HAVING
CIRCULAR STREAMLINES

By Artur Mager and Arthur G. Hansen

SUMMARY

The laminar-boundary-layer development over a semi-infinite flat plate placed in a flow with concentric circular streamlines was investigated with the limitation of small total turning of the main-stream flow. The shape of the velocity profiles in the direction of the main-stream flow and perpendicular to it was analytically determined for an incompressible flow and a compressible flow with Prandtl number equal to 1.

The boundary-layer thickness was shown to be proportional to the square root of the distance from the leading edge of the plate when measured along the streamline of the main-stream flow. The deflection of the boundary-layer flow at the plate surface from the direction of a circular streamline in the main flow was shown to vary directly with the turning. With increase in the Mach number of the main-stream flow, both the boundary-layer thickness and the deflection increased.

INTRODUCTION

The relative lack of theories explaining the behavior of boundary layer when a lateral curvature of the main-stream flow exists has been especially apparent in the application of aerodynamics to the design of turbomachinery. The development of the boundary layer in such cases is strongly influenced by the corresponding normal pressure gradient toward the center of curvature, giving rise to a component of "secondary flow" in the boundary layer. For the laminar case, most of the published work has been restricted to yawed cylinders, wings, and cones (references 1 to 4). One notable exception of direct application to the design of compressors and turbines is reference 5, wherein the boundary layer on a rotating blade is analyzed. For the turbulent case, a general but approximate solution of the momentum-integral equations based on an assumed velocity distribution and friction law is obtained in reference 6.

Aside from the conventional boundary-layer approach to this problem, a number of investigators (references 7 to 9) have obtained solutions for secondary flow arising from flows of varying total pressure or varying enthalpy by neglecting the influence of viscosity but admitting the existence of vorticity. Although such procedure obviously does not permit satisfaction of all the boundary conditions (because the order of the general differential equations for the flow is reduced), the results so obtained give a fair check with the experimental data, except in the regions close to the wall. Thus the indications are that, while it is possible to obtain a fair picture of three-dimensional flows in the preceding cases by neglecting viscosity, such procedures are inadmissible where thin boundary layers exist.

The object of this investigation, which was conducted at the NACA Lewis laboratory, is to solve a case somewhat analogous to that of references 7 to 9 in regard to main-flow orientation while retaining the usual Prandtl boundary-layer assumptions, and thus to demonstrate the influence of viscosity and compressibility on the secondary flow in relatively thin boundary layers.

To this end, the main flow outside the boundary layer is assumed to follow concentric circular streamlines in planes parallel to a semi-infinite flat plate and to be uniform in a direction perpendicular to the plate. The edge of the plate is placed so as to coincide with a radial line through the axis of the main flow (fig. 1). It is assumed, of course, that in the established main-stream flow the effect of viscosity is negligible. In the simplification of the equations for the flow, it was found convenient to follow the procedure first used by Moore (reference 4).

Although the solution is primarily of theoretical interest, it may have some direct bearing on the understanding of secondary flows over a portion of the hub between the compressor guide vanes where the boundary layer is probably still thin and laminar, and where the main flow undergoes relatively little turning, often along a circular path. Here again the analysis would probably be applicable only in regions where boundary-layer flows from the blade surfaces and other "wall effects" were not influential.

BASIC EQUATIONS

The following equations describe the motion of a compressible viscous fluid in vector form (reference 10):

Conservation of mass

$$\frac{D\rho}{Dt} + \rho(\nabla \cdot \bar{q}) = 0 \quad (1)$$

Conservation of momentum

$$\rho \frac{D\bar{q}}{Dt} = \rho \bar{f} - \nabla p + \mu \nabla^2 \bar{q} + \frac{1}{3} \mu \nabla (\nabla \cdot \bar{q}) + 2 \left[(\nabla \mu) \cdot \nabla \right] \bar{q} + (\nabla \mu) \times (\nabla \times \bar{q}) - \frac{2}{3} (\nabla \cdot \bar{q}) (\nabla \mu) \quad (2)$$

Conservation of energy

$$\rho \frac{DE}{Dt} + p(\nabla \cdot \bar{q}) = \Lambda + \nabla \cdot \left[(k \nabla) T \right] \quad (3)$$

where the dissipation function is given by

$$\Lambda = \mu \left\{ 2 \nabla \cdot \left[(\bar{q} \cdot \nabla) \bar{q} \right] + (\nabla \times \bar{q})^2 - 2 \bar{q} \cdot \nabla (\nabla \cdot \bar{q}) - \frac{2}{3} (\nabla \cdot \bar{q})^2 \right\}$$

Equation of state

$$p = \rho R T \quad (4)$$

(All symbols are defined in the appendix.)

When dealing with problems involving a lateral curvature of the potential flow it is convenient to use an orthogonal coordinate system illustrated in figure 2. This system is characterized by a fixed reference axis x of arbitrary curvature $c = c(x)$ and is related to a Cartesian system X_1 as follows:

$$\left. \begin{aligned} x_1 &= \int_0^x \cos \beta \, dx + z \sin \beta \\ x_2 &= y \\ x_3 &= \text{constant} + z \cos \beta - \int_0^x \sin \beta \, dx \end{aligned} \right\} \quad (5)$$

where

$$c = \frac{d\beta}{dx}$$

$$\beta = \beta(x)$$

The elements of length at (x, y, z) in the direction of the increasing coordinates are

$$h_1 dx \quad h_2 dy \quad h_3 dz$$

and their values may be obtained by use of equations (5) as

$$h_1 = (1 + cz)$$

$$h_2 = 1$$

$$h_3 = 1$$

The transformation of equations (1), (2), and (3) from the Cartesian system to the orthogonal system is readily obtainable by use of the expressions for the elements of length (see, for instance, reference 11 or 12). When the y -axis is assumed perpendicular to the surface over which the flow takes place and the usual Prandtl assumptions about the order of magnitude of various terms are made, the equations (1), (2), and (3) take the following form for steady flow in a boundary layer where equations (6), (7), and (8) correspond to equations (1), (2), and (3), respectively:

$$\left\{ \frac{\partial}{\partial x} (\rho u) + \frac{\partial}{\partial y} [(1 + cz)\rho v] + \frac{\partial}{\partial z} [(1 + cz)\rho w] \right\} = 0 \quad (6)$$

$$\rho \left(\frac{u}{1 + cz} \frac{\partial u}{\partial x} + v \frac{\partial u}{\partial y} + w \frac{\partial u}{\partial z} + \frac{c}{1 + cz} uw \right) = - \frac{1}{1 + cz} \frac{\partial p}{\partial x} + \frac{\partial}{\partial y} \left(\mu \frac{\partial u}{\partial y} \right) \quad (7a)$$

$$\rho \left(\frac{u}{1 + cz} \frac{\partial w}{\partial x} + v \frac{\partial w}{\partial y} + w \frac{\partial w}{\partial z} - \frac{c}{1 + cz} u^2 \right) = - \frac{\partial p}{\partial z} + \frac{\partial}{\partial y} \left(\mu \frac{\partial w}{\partial y} \right) \quad (7b)$$

Concomitant with (7a) and (7b) is the result that $\frac{\partial p}{\partial y}$ is of order of magnitude $\delta \approx 0$.

$$\rho \left(\frac{u}{1 + cz} \frac{\partial E}{\partial x} + v \frac{\partial E}{\partial y} + w \frac{\partial E}{\partial z} \right) = - \frac{p}{1 + cz} \left\{ \frac{\partial u}{\partial x} + \frac{\partial}{\partial y} [(1 + cz)v] + \frac{\partial}{\partial z} [(1 + cz)w] \right\} + \mu \left[\left(\frac{\partial u}{\partial y} \right)^2 + \left(\frac{\partial w}{\partial y} \right)^2 \right] + \frac{\partial}{\partial y} \left(k \frac{\partial T}{\partial y} \right) \quad (8)$$

The equation of state (4) remains unchanged.

Because of the nature of the problem under consideration, several simplifications in the preceding equations can be made. First, the fixed reference axis x will be chosen to coincide with a streamline of the main-stream flow where these streamlines are assumed to be arcs of concentric circles in planes parallel to a semi-infinite flat plate (see fig. 1). This flat plate is oriented so that its leading edge is orthogonal to the reference axis x ; hence the leading edge can be defined by $x = 0$, $y = 0$. Secondly, if the velocity of the fluid in the main stream is designated u_1 , it follows that $u_1 = \text{constant}$ along any given streamline; that is, $u_1 = u_1(z)$.

It also follows from the nature of the prescribed main-stream flow that the pressure gradient in the x -direction and outside the boundary layer is identically zero. In view of the order of magnitude of $\partial p / \partial y$, the same pressure prevails in the boundary layer as in the main flow, and consequently (where the subscript indicates partial differentiation)

$$p_x = 0 \quad (9)$$

In addition, for flow with circular streamlines it may be shown that

$$p_z = \left(\frac{c}{1 + cz} \right) \rho_1 u_1^2 \quad (10)$$

The boundary conditions on equations (6) and (7) are

$$\left. \begin{aligned} u(x, \infty, z) &= u_1(z) \\ w(x, \infty, z) &= 0 \\ u(x, 0, z) &= w(x, 0, z) = v(x, 0, z) = 0 \end{aligned} \right\}$$

where

$$x > 0$$

and at the leading edge

$$\left. \begin{aligned} u(0, y, z) &= u_1 \\ w(0, y, z) &= v(0, y, z) = 0 \end{aligned} \right\}$$

where

$$y > 0$$

(11)

For equation (8), usually two boundary conditions on temperature are used by defining its value at $y = 0$ and $y \rightarrow \infty$. For the case under consideration, however, it will be necessary to define temperature only at $y = 0$.

SOLUTION OF EQUATIONS

Application of Vector Potential Concept

In order to satisfy the equation of continuity (6) and to eliminate one dependent variable from equations (7), the concept of a vector potential is employed (see reference 4). To this end, two functions ψ and ϕ are defined, where

$$\left. \begin{aligned} \rho u &\equiv \psi_y \\ (1 + cz)\rho w &\equiv \varphi_y \\ (1 + cz)\rho v &\equiv -(\psi_x + \varphi_z) \end{aligned} \right\} \quad (12)$$

It may be verified by direct substitution of equations (12) into equation (6) that equation (6) is identically satisfied.

Substitution of equations (9), (10), and (12) into equations (7a) and (7b) yields

$$\begin{aligned} \psi_y \left(\frac{\psi_y}{\rho} \right)_x + \varphi_y \left(\frac{\psi_y}{\rho} \right)_z - (\psi_x + \varphi_z) \left(\frac{\psi_y}{\rho} \right)_y + \frac{c}{1 + cz} \psi_y \left(\frac{\varphi_y}{\rho} \right) \\ = (1 + cz) \left[\mu \left(\frac{\psi_y}{\rho} \right)_y \right]_y \end{aligned} \quad (13a)$$

$$\begin{aligned} \psi_y \left[\frac{\varphi_y}{\rho(1 + cz)} \right]_x + \left[\frac{\varphi_y}{(1 + cz)} \right] \left(\frac{\varphi_y}{\rho} \right)_z - (\psi_x + \varphi_z) \left[\frac{\varphi_y}{\rho(1 + cz)} \right]_y - \frac{c}{\rho} (\psi_y)^2 - \\ \frac{c}{(1 + cz)^2} \frac{\varphi_y^2}{\rho} = -c\rho_1 U_1^2 + \left[\mu \left(\frac{\varphi_y}{\rho} \right)_y \right]_y \end{aligned} \quad (13b)$$

Incompressible Case

The solution for the incompressible flow ($\rho = \text{constant}$) will be presented first. For this case it is necessary to consider only equations (13) in the boundary layer; the energy equation need not be used.

In accordance with the usual procedure in the solution of incompressible boundary-layer flows, the following substitutions for the variables are employed:

$$\left. \begin{aligned} \eta &= y \sqrt{\frac{u_1}{\nu x(1+zc)}} \\ \psi &= \rho \sqrt{x\nu u_1(1+zc)} F(\eta) \\ \phi &= \rho c x (1+zc) \sqrt{x\nu u_1(1+zc)} G(\eta) \end{aligned} \right\} \quad (14)$$

The following system of equations is obtained by substituting expressions (14) along with their appropriate partial derivatives into equations (13) (note that $\mu/\rho = \nu$):

$$\begin{aligned} & (cx)^2 G'F' \left[\frac{(1+zc)}{u_1 c} \frac{du_1}{dz} + 1 \right] - \\ & (cx)^2 F''G \left[\frac{3}{2} + \frac{(1+zc)}{2cu_1} \frac{du_1}{dz} \right] - \frac{FF''}{2} - F'''' = 0 \end{aligned} \quad (15a)$$

$$\begin{aligned} & F'G' - \frac{FG''}{2} + (1 - F'^2) - G'''' + (cx)^2 G'^2 \left[\frac{(1+zc)}{cu_1} \frac{du_1}{dz} \right] - \\ & (cx)^2 G''G \left[\frac{3}{2} + \frac{(1+zc)}{2cu_1} \frac{du_1}{dz} \right] = 0 \end{aligned} \quad (15b)$$

It is interesting to note that setting

$$u_1 = u_{1,0}(1+zc)^n \quad (16)$$

in (15a) and (15b) reduces these equations, respectively, to the forms

$$(cx)^2 G'F' (n+1) + (cx)^2 F''G \left(\frac{3}{2} + n \right) - \frac{FF''}{2} - F'''' = 0 \quad (17a)$$

$$\begin{aligned} & n(cx)^2 (G')^2 - (cx)^2 G''G \left(\frac{3}{2} + n \right) + F'G' - \frac{FG''}{2} + (1 - F'^2) - G'''' = 0 \\ & \hspace{25em} (17b) \end{aligned}$$

Letting $n = -1$ in equation (16) gives the expression for the velocity in the classical irrotational vortex flow, whereas letting $n = 1$ yields the expression for a special case of "wheel-type" flow.

Now F and G and their derivatives are assumed of order of magnitude of unity, while $(cx)^2 \ll 1$. It is seen that cx is the total turning of the flow outside the boundary layer, and because of the foregoing restriction it must remain small. It is further assumed that

$\left(\frac{1 + zc}{cu_1} \frac{du_1}{dz} \right)$ is of the order of magnitude of unity (which should be the case for most flows of interest and is evidenced in part by equation (16)). Neglecting all terms of the order of $(cx)^2$ in equations (15) and (17) reduces these equations to the following two total differential equations:

$$FF'' + 2F''' = 0 \quad (18a)$$

$$2F'G' - FG'' - 2G''' + 2[1 - (F')^2] = 0 \quad (18b)$$

The corresponding boundary conditions are

$$\left. \begin{array}{l} F = F' = G = G' = 0 \text{ at } \eta = 0 \\ \text{and} \\ F' = 1 \text{ and } G' = 0 \text{ as } \eta \rightarrow \infty \end{array} \right\} \quad (19)$$

Equations (18) and (19) show that for small turning F is the usual Blasius function and that equation (18b) may be solved for G' (or G) since F is known. Such solution was obtained by relaxation procedure inasmuch as F and its derivatives are given in tabular form only (cf. reference 13, p. 121). The results from this computation are presented in figure 3 and table I.

Boundary-layer thickness. - If the boundary-layer thickness δ is defined as the value of y at which u is a certain percentage of u_1 (usually over 99 percent), a corresponding value for η may be found from the solution for F where this value of η is designated η^* . Consequently the expression for boundary-layer thickness may be obtained from equations (14) as

$$\delta = \eta^* \sqrt{1 + cz} \sqrt{\frac{v_x}{u_1}} \quad (20)$$

or nondimensionally in terms of the reference length x as

$$\frac{\delta}{x} = \eta^* \sqrt{1 + cz} \operatorname{Re}^{-\frac{1}{2}} \quad (21)$$

On a given streamline, it can be seen from equation (20) that the boundary-layer thickness varies directly with the square root of x . For the special case of free vortex flow, equation (20) becomes

$$\delta = \eta^* (1 + cz) \sqrt{\frac{vx}{u_{1,0}}} \quad (22)$$

and it follows that for any given x and $u_{1,0}$, thickness increases in proportion to $(1 + cz)$ or that the boundary layer becomes thinner with an increase in curvature of the flow. The lines of constant thickness are obtained by considering δ to be a constant in equation (22), or

$$x = \frac{\text{constant}}{(1 + cz)^2} \quad (23)$$

Therefore, the curves of constant δ are spirals of lituus; they are shown in figure 4. For more general flows, the lines of constant boundary-layer thickness are given by

$$x = \frac{u_1 (\text{constant})}{(1 + cz)}$$

where, of course, u_1 is a function of $(1 + cz)$.

Flow direction at plate surface. - From equations (12) and (14) the expressions for u and w are

$$u = u_1 F'$$

$$w = cxu_1 G'$$

Therefore, if

$$\epsilon = \lim_{\eta \rightarrow 0} \frac{w}{u}$$

the flow direction at the plate is given by

$$\alpha = \arctan \epsilon \quad (24)$$

However, since $G'(0) = F'(0) = 0$,

$$\epsilon = cx \frac{G''(0)}{F''(0)} \quad (25)$$

Equation (25) indicates that

$$\tau_{0,z} = \epsilon \tau_{0,x}$$

inasmuch as

$$\tau_{0,x} = \left. \frac{\mu \partial u}{\partial y} \right|_{(y=0)}$$

$$\tau_{0,z} = \left. \frac{\mu \partial w}{\partial y} \right|_{(y=0)}$$

The ratio $G''(0)/F''(0)$ was evaluated numerically to give the result

$$\epsilon = -3.26 \, cx$$

It may be seen, then, that at the plate surface the flow is deflected from the direction of the streamline toward the center of curvature of the main-stream flow and that this deflection is proportional to the turning. The lines of constant ϵ are seen from equation (25) to be those of constant turning, that is, radial lines (see fig. 4).

Effect of Compressibility

Complexity prevents the extension of the previous results to include the effects of compressibility in the same manner as for the incompressible case. For compressible flow, a solution can be obtained only in the immediate neighborhood of a reference streamline on which the Mach number has been specified. However, it is possible to calculate the Mach numbers on various chosen streamlines in terms of the Mach number specified on an initial streamline. Solutions can then be found in the neighborhood of the chosen streamlines using the calculated Mach numbers. To find the boundary-layer flow in any region of interest is therefore possible.

Simplification of energy equation. - Letting $\theta = C_p T$ and assuming that the specific heats and Prandtl number are constant, the energy equation can be written in terms of φ and ψ as

$$\psi_y \theta_x + \varphi_y \theta_z - (\psi_x + \varphi_z) \theta_y = \frac{c}{1 + cz} U_1^2 \varphi_y + (1 + cz) \mu \left(\left[\left(\frac{\psi_y}{\rho} \right)_y \right]^2 + \left\{ \left[\frac{\varphi_y}{\rho(1 + cz)} \right]_y \right\}^2 \right) \quad (26)$$

For Prandtl number equal to 1 and zero heat transfer at the plate surface, equation (26) is replaced by

$$C_p T + \frac{1}{2} \left\{ \left(\frac{\psi_y}{\rho} \right)^2 + \left[\frac{\varphi_y}{\rho(1 + cz)} \right]^2 \right\} = T_w C_p \quad (27)$$

where T_w is the constant temperature of the plate.

Reduction of equations to nondimensional form. - The following approximate formula (reference 14) is used to represent the relation between the viscosity and the temperature:

$$\frac{\mu}{\mu_{1,0}} = A \frac{T}{T_{1,0}} \quad (28)$$

where A is a constant suitably adjusted to give the best agreement with the actual relation over the temperature range considered.

It now becomes convenient to make all physical quantities in the various equations nondimensional. The following system suggested in reference 4 will be used; all quantities on the left are to be considered relative to the quantities on the right, which are measured outside the boundary layer and along the reference axis x :

u, v, w	relative to $u_{1,0}$
$x, y, z, \frac{1}{c}$	relative to $\mu_{1,0} A / \rho_{1,0} u_{1,0}$
ρ	relative to $\rho_{1,0}$
T	relative to $u_{1,0}^2 / 2C_p$

p relative to $\rho_{1,0} u_{1,0}^2$

ψ, φ relative to $\mu_{1,0} A$

All subsequent equations will appear in nondimensional form. As a consequence of the use of the nondimensional form, equation (13a) becomes

$$\begin{aligned} \psi_y \left(\frac{\psi_y}{\rho} \right)_x + \varphi_y \left(\frac{\psi_y}{\rho} \right)_z - (\psi_x + \varphi_z) \left(\frac{\psi_y}{\rho} \right)_y + \frac{c}{1 + cz} \psi_y \left(\frac{\varphi_y}{\rho} \right) \\ = (1 + cz) \left[\frac{T}{T_{1,0}} \left(\frac{\psi_y}{\rho} \right)_y \right]_y \end{aligned}$$

equation (13b) becomes

$$\begin{aligned} \psi_y \left[\frac{\varphi_y}{\rho(1 + cz)} \right]_x + \frac{\varphi_y}{(1 + cz)} \left(\frac{\varphi_y}{\rho} \right)_z - (\psi_x + \varphi_z) \left[\frac{\varphi_y}{\rho(1 + cz)} \right] - \\ \frac{c}{\rho} (\psi_y)^2 - \frac{c}{(1 + cz)^2} \frac{\varphi_y^2}{\rho} = -c\rho_1 u_1^2 + \left[\frac{T}{T_{1,0}} \left(\frac{\varphi_y}{\rho} \right)_y \right]_y \end{aligned}$$

equation (27) becomes

$$T + \left\{ \left(\frac{\psi_y}{\rho} \right)^2 + \left[\frac{\varphi_y}{\rho(1 + cz)} \right]^2 \right\} = T_w$$

and equation (4) will be written

$$\frac{p_1}{p_{1,0}} = \rho \frac{T}{T_{1,0}} \quad (29)$$

Transformation of Howarth. - The following transformation of variables indicated by Howarth (reference 15) is now utilized to make the nondimensional form of equations (13a) and (13b) similar to the incompressible form of these equations:

$$\left. \begin{aligned} Y &\equiv \left(\frac{p_1}{p_{1,0}} \right)^{-\frac{1}{2}} \int_0^y \rho dy \\ X &\equiv x \\ Z &\equiv z \\ \psi &\equiv \left(\frac{p_1}{p_{1,0}} \right)^{\frac{1}{2}} \Psi \\ \phi &\equiv \left(\frac{p_1}{p_{1,0}} \right)^{\frac{1}{2}} \Phi \end{aligned} \right\} \quad (30)$$

As a consequence of transformations (30), equation (29), and the fact that $\partial p / \partial y$ is of the order of magnitude δ , equations (13a), (13b), and (27) become, respectively:

$$\begin{aligned} &\Psi_Y \Psi_{YX} + \Phi_Y \Psi_{YZ} - (\Psi_X + \Phi_Z) \Psi_{YY} + \frac{c}{1 + cZ} \Psi_Y \Phi_Y \\ &= \Psi_{YY} \left(\frac{c}{1 + cZ} \frac{u_1^2}{2} \frac{T_{1,0}}{T_1} \frac{1}{p_{1,0}} \Phi \right) + (1 + cZ) \Psi_{YYY} \end{aligned} \quad (31a)$$

$$\begin{aligned} &\Psi_Y \Phi_{YX} + \Phi_Y \Phi_{YZ} - (\Psi_X + \Phi_Z) \Phi_{YY} - \frac{c}{1 + cZ} (\Phi_Y)^2 + c(1 + cZ) \left[\frac{p_1}{\rho} u_1^2 - (\Psi_Y)^2 \right] \\ &= \frac{c}{1 + cZ} \frac{u_1^2}{2} \frac{T_{1,0}}{T_1} \frac{\Phi}{p_{1,0}} \Phi_{YY} + (1 + cZ) \Phi_{YYY} \end{aligned} \quad (31b)$$

$$T + (\Psi_Y)^2 + \left(\frac{\Phi_Y}{1 + cZ} \right)^2 = T_w \quad (32)$$

The same procedure as for the incompressible flow case is now followed. The similarity variable and corresponding vector potential components are defined as

$$\left. \begin{aligned} \bar{\eta} &= Y \sqrt{\frac{u_1}{X(1+Zc)}} \\ \Psi &= \sqrt{Xu_1(1+Zc)} \quad \bar{F}(\eta) \\ \Phi &= cX(1+Zc) \sqrt{Xu_1(1+Zc)} \quad \bar{G}(\eta) \end{aligned} \right\} \quad (33)$$

By use of these definitions, equations (31) become

$$\begin{aligned} (cx)^2 \bar{G}' \bar{F}' \left[1 + \frac{(1+Zc)}{cu_1} \frac{du_1}{dz} \right] + (cx)^2 \bar{G} \bar{F}'' \left[\frac{\gamma}{2} M_1^2 - \frac{3}{2} - \right. \\ \left. \frac{(1+Zc)}{2cu_1} \frac{du_1}{dz} \right] - \frac{\bar{F} \bar{F}''}{2} - \bar{F}'^3 = 0 \end{aligned} \quad (34a)$$

$$\begin{aligned} \bar{F}' \bar{G}' - \frac{\bar{F} \bar{G}''}{2} + \left(1 + \frac{\gamma-1}{2} M_1^2 \right) (1 - \bar{F}'^2) - \bar{G}'^3 + \\ (cx)^2 \bar{G}'^2 \left[\frac{(1+Zc)}{cu_1} \frac{du_1}{dz} - \frac{\gamma-1}{2} M_1^2 \right] - (cx)^2 \bar{G}'' \bar{G} \left[\frac{3}{2} + \frac{(1+Zc)}{2cu_1} \frac{du_1}{dz} + \frac{\gamma}{2} M_1^2 \right] = 0 \end{aligned} \quad (34b)$$

Boundary conditions are the same as in equations (19) with the appropriate change in variables; that is

$$\bar{F} = \bar{F}' = \bar{G} = \bar{G}' = 0 \quad \text{at} \quad \bar{\eta} = 0$$

and

$$\bar{F}' = 1 \quad \text{and} \quad \bar{G}' = 0 \quad \text{as} \quad \bar{\eta} \rightarrow \infty$$

Once again when terms of the order of magnitude of $(cx)^2$ are eliminated under the same type of restrictions as in the incompressible case, equation (34a) becomes the Blasius equation for \bar{F} . However, it

may be seen that equation (34b) cannot be solved directly as a total differential equation in $\bar{\eta}$ since M_1 is a function of Z . In fact, if u_1 is specifically prescribed as a function of $(1 + cz)$ (that is, $u_1 = f(1 + cz)$ where $f = 1$ when $z = 0$), then M_1 may be expressed as

$$M_1^2 = \frac{M_{1,0}^2 f^2}{\left[\frac{\gamma-1}{2} M_0^2 (1 - f^2) + 1 \right]} \quad (35)$$

and in the immediate neighborhood of the reference axis X , $M_1 \approx M_{1,0}$ and may be considered a constant. Incorporating the preceding restrictions into equation (34b) gives

$$\bar{F}'\bar{G}' - \bar{G}''' - 1/2 \bar{F}\bar{G}'' + \left(1 + \frac{\gamma-1}{2} M_{1,0}^2 \right) \left[1 - (\bar{F}')^2 \right] = 0 \quad (36)$$

This equation has the solution

$$\bar{G}' = \left(1 + \frac{\gamma-1}{2} M_{1,0}^2 \right) G'(\bar{\eta}) \quad (37)$$

where G' is known from the incompressible case. Curves of $\bar{G}'(\bar{\eta})$ for various values of $M_{1,0}$ are plotted in figure 5.

As mentioned previously, the flow in the neighborhood of streamlines other than an initial reference streamline may be calculated in the same manner by taking the reference axis along the new streamline and by computing the appropriate Mach number on this streamline from equation (35).

Physical coordinates. - Relations (29), (30), and (32) may be used to obtain values of y as a function of $\bar{\eta}$ for a fixed value of x

$$y = (x)^{1/2} \left\{ \bar{\eta} + \left[\bar{\eta} - \int_0^{\bar{\eta}} (\bar{F}')^2 d\bar{\eta} \right] \frac{\gamma-1}{2} M_{1,0}^2 \right\} \quad (38)$$

It is to be recalled, of course, that these coordinates are the non-dimensional form of the true physical coordinates.

Interpretation of results. - From equations (18), (36), and (38), the effect of compressibility may be seen to be twofold, namely, changes occur in the coordinate y as a function of η and the differential equation for G . These changes have a corresponding influence on the velocity distribution, the boundary-layer thickness, and the flow deflection at the plate surface.

Since $\left[\bar{\eta} - \int_0^{\bar{\eta}} (\bar{F}')^2 d\bar{\eta} \right]$ is a positive function of $\bar{\eta}$, for any given value of $\bar{\eta}$ the value of y increases with Mach number, as shown by equation (38). Consequently, the boundary-layer thickness δ increases with Mach number. It also follows for a chosen Mach number that

$$\frac{\partial u}{\partial y} = (x)^{1/2} \left[1 + \frac{\gamma-1}{2} M_{1,0}^2 (1 - \bar{F}'^2) \right] \frac{du}{d\bar{\eta}}$$

thereby indicating that $\partial u / \partial y$ increases with Mach number for $\eta = \text{constant}$. The same effect is known to exist in two-dimensional boundary-layer flow.

As far as the flow deflection at the plate surface is concerned, the changes in the shape of \bar{G}' (see fig. 5) and equation (25) indicate that for a given turning the deflection toward the center of the flow field increases with Mach number. Consequently, larger secondary flows in the boundary layer are obtained with the increase in Mach number.

CONCLUSIONS

The following conclusions were drawn from a theoretical investigation of boundary-layer flow over a flat plate when the main-stream flow outside the boundary layer follows concentric circular streamlines and the total turning of that flow is small:

1. The profile of the velocity component in the direction of the flow outside the boundary layer is identical to that existing in two-dimensional flow over a flat plate.
2. The magnitude of the velocity component in the direction perpendicular to the flow outside the boundary layer and in a plane parallel to the plate varies directly with the turning of the main-stream flow.
3. The boundary-layer thickness varies with the square root of the distance along the streamline of the main-stream flow as measured from the leading edge of the plate. For the special case of free vortex flow, the lines of constant boundary-layer thickness are spirals of lituus.
4. The deflection of the flow at the plate surface from the direction of the main-stream flow is directly proportional to the turning of the main-stream flow. The lines of constant deflection are therefore radial.

5. Both the boundary-layer thickness and the deflection at the plate surface increase with Mach number. Consequently, larger secondary flows in the boundary layer are obtained for higher Mach numbers.

Lewis Flight Propulsion Laboratory
National Advisory Committee for Aeronautics
Cleveland, Ohio, November 27, 1951

APPENDIX - SYMBOLS

The following symbols are used in this report:

A	constant in viscosity-temperature relation
C_p	specific heat at constant pressure process
c	curvature of x -axis, $d\beta/dx$
$\frac{D}{Dt}$	Eulerian derivative
∇	vector differential operator
E	energy
$\left. \begin{matrix} F, \bar{F} \\ G, \bar{G} \end{matrix} \right\}$	functions related to components of vector potential
\bar{f}	inertial field force
h_i	factor used in transformation of coordinates ($i = 1, 2, 3$)
k	thermal conductivity
M	Mach number
p	pressure
\bar{q}	velocity vector
R	gas constant
Re	Reynolds number based on x , $(u_1 x / \nu)$
T	temperature
u, v, w	velocity components in curvilinear coordinate system
X, Y, Z	coordinates defined by equation (30)
x, y, z	curvilinear coordinates
α	boundary-layer deflection angle measured from direction of flow at plate surface to direction of flow outside boundary layer

β	angle between X_1 -axis and tangent to x -axis
γ	ratio of specific heats
δ	boundary-layer thickness
ϵ	measure of boundary-layer deflection near plate surface, $\tan \alpha$
$\eta, \bar{\eta}$	similarity variables
η^*	value of η at $y = \delta$
θ	enthalpy, $c_p T$
Λ	dissipation function
μ	absolute viscosity
ν	kinematic viscosity, μ/ρ
ρ	density
$\tau_{0,x}, \tau_{0,z}$	shear stress at wall in x - and z -directions, respectively
$\left. \begin{matrix} \Phi, \varphi \\ \Psi, \psi \end{matrix} \right\}$	components of vector potential
X_i	Cartesian coordinates ($i = 1, 2, 3$)
Subscripts:	
l	outside the boundary layer
0	on reference axis x
w	at plate surface

All other subscripts indicate partial differentiation.

Superscript primes indicate total differentiation.

REFERENCES

1. Prandtl, L.: On Boundary Layers in Three-Dimensional Flow. Reps. & Trans. No. 64, British M.A.P., May 1, 1946.
2. Sears, W. R.: The Boundary Layer of Yawed Cylinders. Jour. Aero. Sci., vol. 15, no. 1, Jan. 1948, pp. 49-52.
3. Wild, J. M.: The Boundary Layer of Yawed Infinite Wings. Jour. Aero. Sci., vol. 16, no. 1, Jan. 1949, pp. 41-45.
4. Moore, Franklin K.: Three-Dimensional Compressible Laminar Boundary-Layer Flow. NACA TN 2279, 1951.
5. Fogarty, Laurence Eugene: The Laminar Boundary Layer on a Rotating Blade. Jour. Aero. Sci., vol. 18, no. 4, April 1951, pp. 247-252.
6. Mager, Artur: Generalization of Boundary-Layer Momentum-Integral Equations to Three-Dimensional Flows Including Those of Rotating System. NACA TN 2310, 1951.
7. Squire, H. B., and Winter, K. G.: The Secondary Flow in a Cascade of Airfoils in a Nonuniform Stream. Jour. Aero. Sci. vol. 18, no. 4, April 1951, pp. 271-277.
8. Hawthorne, William R.: Secondary Circulation in Fluid Flow. Gas Turbine Lab., M.I.T., May 1950.
9. Kronauer, Richard E.: Secondary Flows in Fluid Dynamics. Pratt and Whitney Res. Rep. No. 132, Gordon McKay Lab., Harvard Univ., April 1951.
10. Cope, W. F., and Hartree, D. R.: The Laminar Boundary Layer in Compressible Flow. Phil. Trans. Roy. Soc. (London), ser. A, vol. 241, no. 827, June 22, 1948, pp. 1-69.
11. Margenau, Henry, and Murphy, George Moseley: The Mathematics of Physics and Chemistry. D. Van Nostrand Co., Inc., 1943, p. 167.
12. Goldstein, Sidney: Modern Developments in Fluid Dynamics. Vol. I., Clarendon Press (Oxford), 1938.
13. Schlichting, H.: Lecture Series "Boundary-Layer Theory". Part I - Laminar Flows. NACA TM 1217, 1949.
14. Chapman, Dean R., and Rubesin, Morris W.: Temperature and Velocity Profiles in the Compressible Laminar Boundary Layer with Arbitrary Distribution of Surface Temperature. Jour. Aero. Sci., vol. 16, no. 9, Sept. 1949, pp. 547-565.

15. Howarth, L.: Concerning the Effect of Compressibility on Laminar Boundary Layers and Their Separation. Proc. Roy. Soc. (London), ser. A, vol. 194, no. A1036, July 28, 1948, pp. 16-42.

TABLE I - VALUES OF $G'(\eta)$

η	$G'(\eta)$	η	$G'(\eta)$
0	0	3.4	-0.174
.2	-.198	3.6	-.137
.4	-.356	3.8	-.106
.6	-.476	4.0	-.081
.8	-.561	4.2	-.060
1.0	-.613	4.4	-.044
1.2	-.638	4.6	-.032
1.4	-.638	4.8	-.022
1.6	-.619	5.0	-.015
1.8	-.585	5.2	-.010
2.0	-.539	5.4	-.006
2.2	-.486	5.6	-.004
2.4	-.430	5.8	-.002
2.6	-.372	6.0	-.001
2.8	-.316	6.2	-.001
3.0	-.264	6.4	-.000
3.2	-.216		



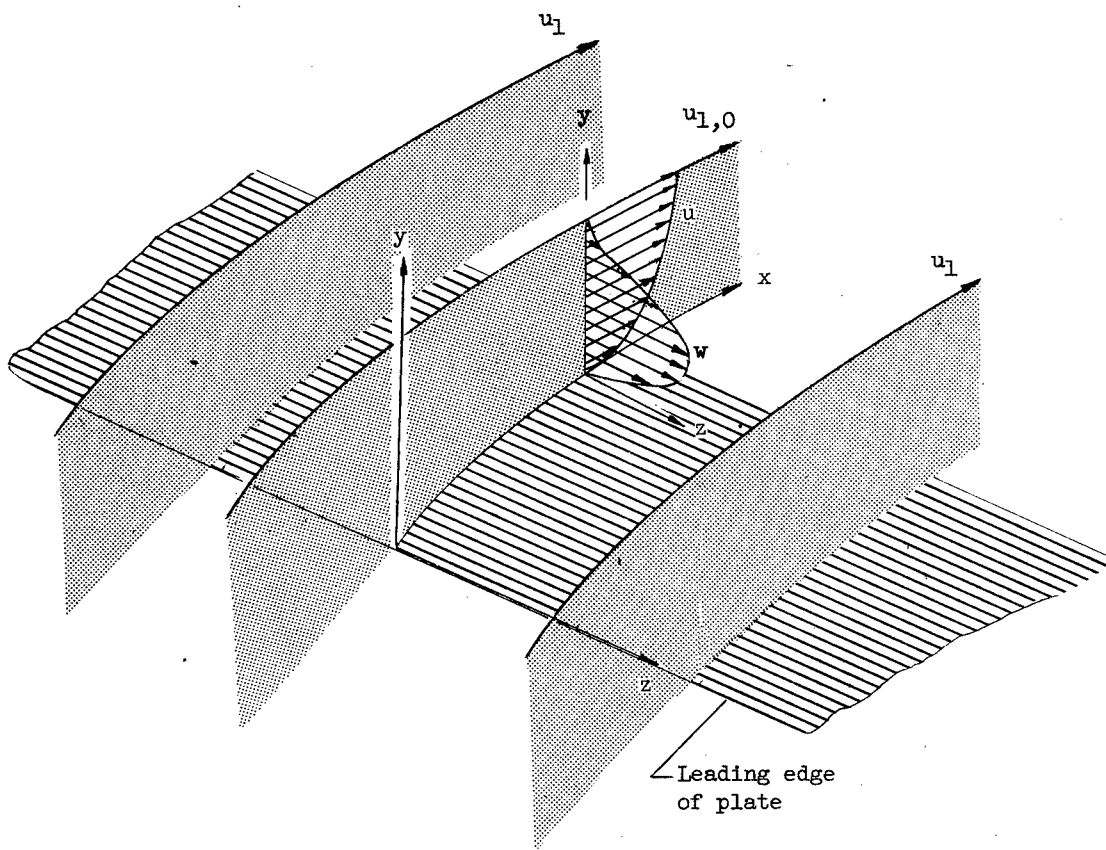


Figure 1. - Flow over plate surface showing streamlines outside boundary layer, orientation of axes, and orientation of velocity components within boundary layer.

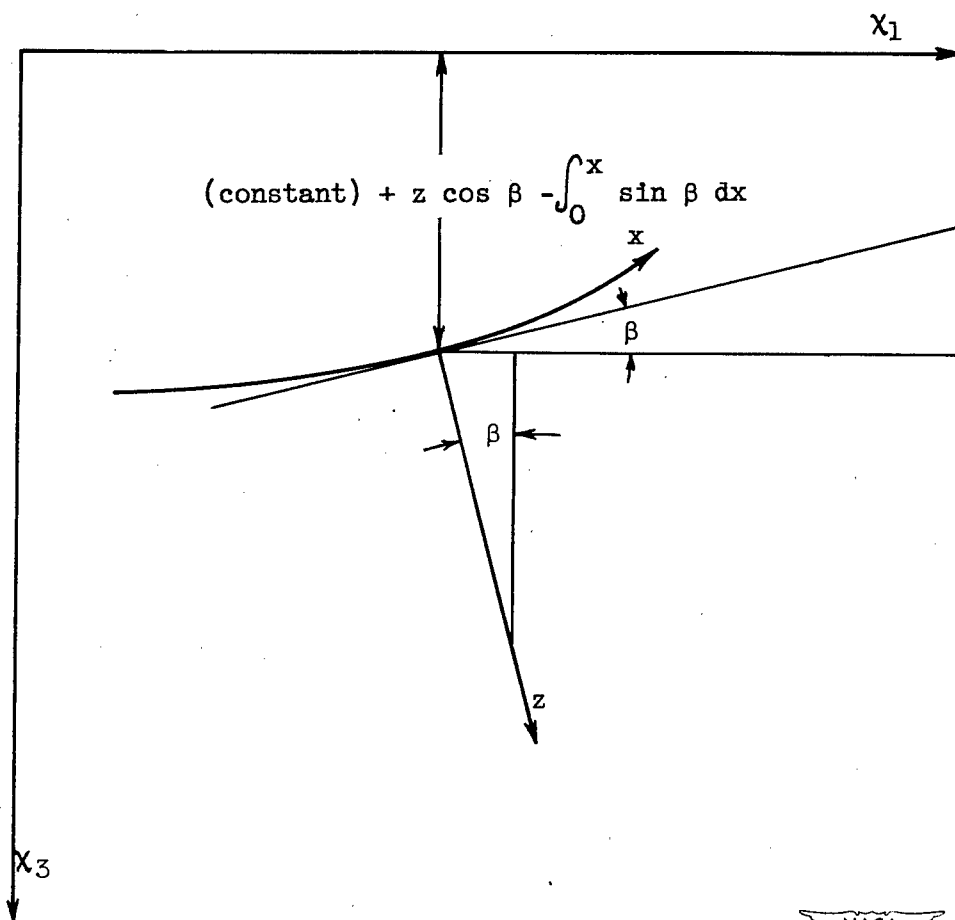


Figure 2. - Transformation from Cartesian coordinates x_1 to curvilinear coordinates x, y, z .

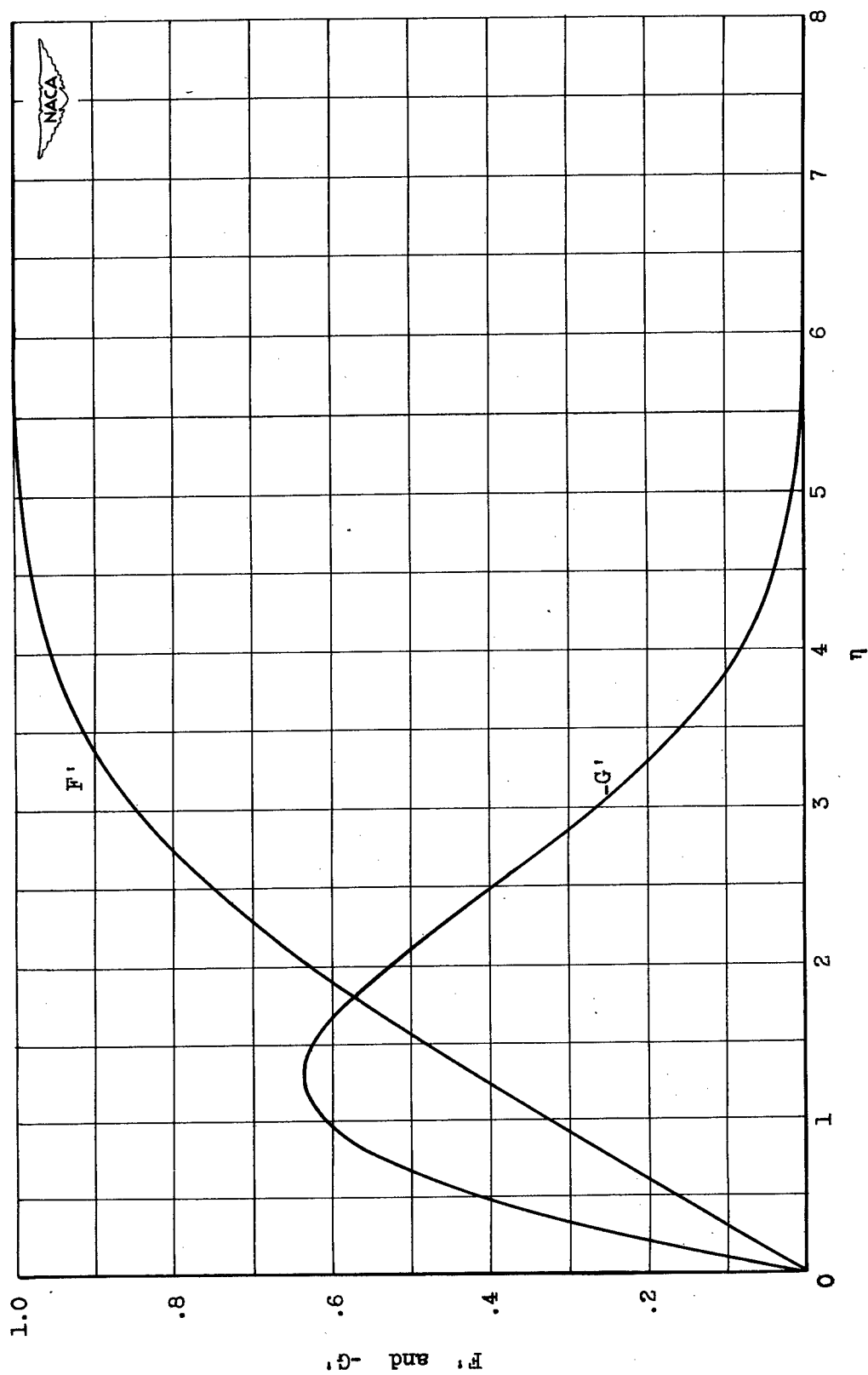


Figure 3. - Functions F' and $-G'$ plotted against η .

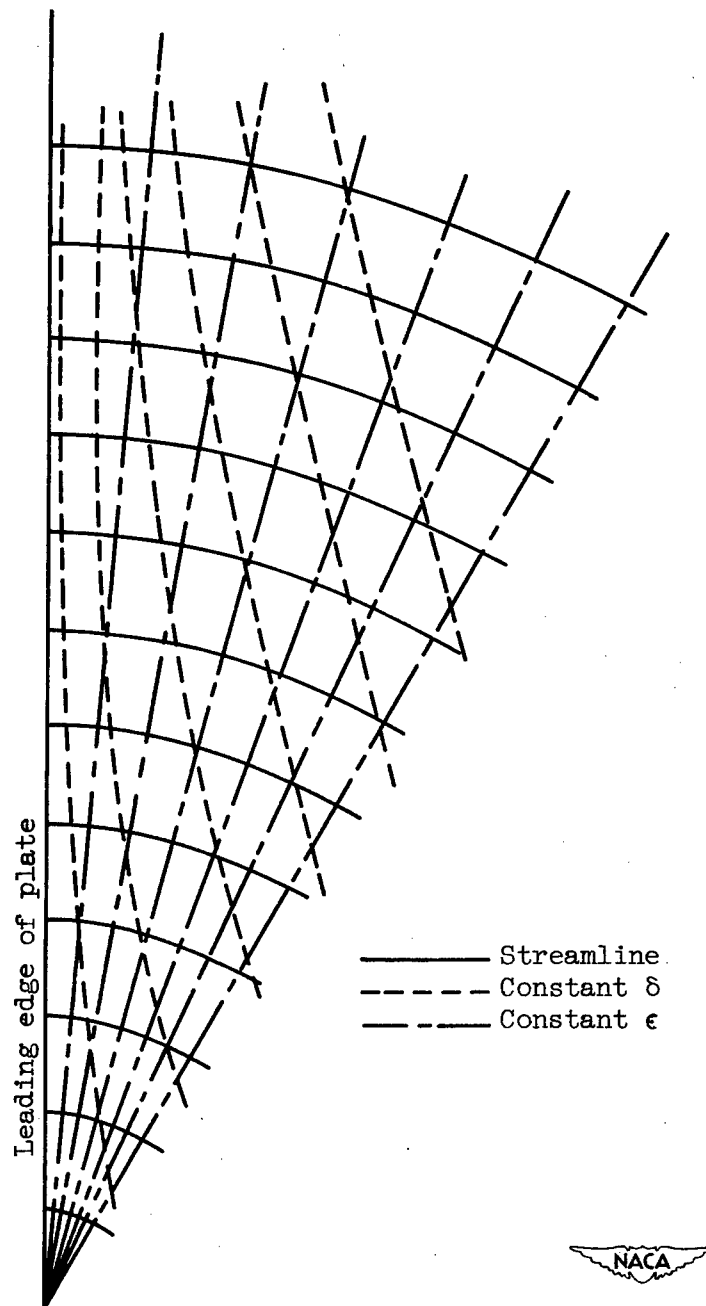


Figure 4. - Lines of constant δ and ϵ
for free vortex flow.

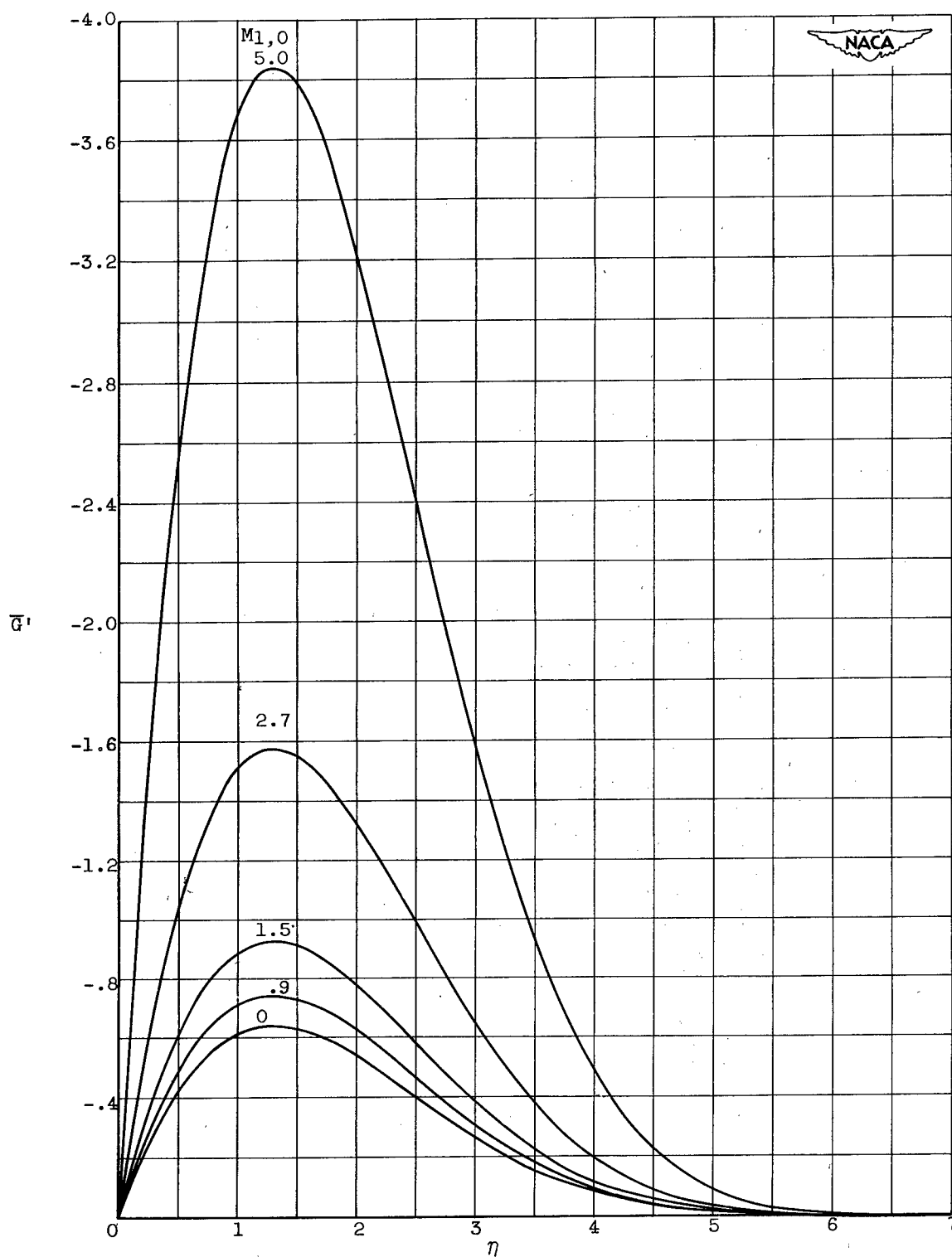






Figure 5. - Effect of Mach number on function \bar{G}' .

<p>NACA TN 2658 National Advisory Committee for Aeronautics. LAMINAR BOUNDARY LAYER OVER FLAT PLATE IN A FLOW HAVING CIRCULAR STREAMLINES. Artur Mager and Arthur G. Hansen. March 1952. 28p. diagrs., tab. (NACA TN 2658)</p> <p>The laminar-boundary-layer development over a semi-infinite flat plate placed in a flow with concentric circular streamlines was investigated with the limitation of small total turning of the main-stream flow. The shape of the velocity profiles in the direction of the main-stream flow and perpendicular to it was analytically determined for an incompressible flow and a compressible flow with Prandtl number equal to 1. The boundary-layer thickness was shown to be proportional to the square root of the distance from the leading edge of the plate when measured along the streamline of the main-stream flow. The deflection of the boundary-layer flow at the plate surface</p> <p>Copies obtainable from NACA, Washington (over)</p>	<p>NACA TN 2658 National Advisory Committee for Aeronautics. LAMINAR BOUNDARY LAYER OVER FLAT PLATE IN A FLOW HAVING CIRCULAR STREAMLINES. Artur Mager and Arthur G. Hansen. March 1952. 28p. diagrs., tab. (NACA TN 2658)</p> <p>The laminar-boundary-layer development over a semi-infinite flat plate placed in a flow with concentric circular streamlines was investigated with the limitation of small total turning of the main-stream flow. The shape of the velocity profiles in the direction of the main-stream flow and perpendicular to it was analytically determined for an incompressible flow and a compressible flow with Prandtl number equal to 1. The boundary-layer thickness was shown to be proportional to the square root of the distance from the leading edge of the plate when measured along the streamline of the main-stream flow. The deflection of the boundary-layer flow at the plate surface</p> <p>Copies obtainable from NACA, Washington (over)</p>	<p>1. Flow, Viscous (1.1.3) 2. Flow, Laminar (1.1.3.1) 3. Boundary-Layer Characteristics - Internal Aerodynamics (1.4.7.1)</p> <p>I. Mager, Artur II. Hansen, Arthur G. III. NACA TN 2658</p> <p style="text-align: center;"></p>	<p>1. Flow, Viscous (1.1.3) 2. Flow, Laminar (1.1.3.1) 3. Boundary-Layer Characteristics - Internal Aerodynamics (1.4.7.1)</p> <p>I. Mager, Artur II. Hansen, Arthur G. III. NACA TN 2658</p> <p style="text-align: center;"></p>
<p>NACA TN 2658 National Advisory Committee for Aeronautics. LAMINAR BOUNDARY LAYER OVER FLAT PLATE IN A FLOW HAVING CIRCULAR STREAMLINES. Artur Mager and Arthur G. Hansen. March 1952. 28p. diagrs., tab. (NACA TN 2658)</p> <p>The laminar-boundary-layer development over a semi-infinite flat plate placed in a flow with concentric circular streamlines was investigated with the limitation of small total turning of the main-stream flow. The shape of the velocity profiles in the direction of the main-stream flow and perpendicular to it was analytically determined for an incompressible flow and a compressible flow with Prandtl number equal to 1. The boundary-layer thickness was shown to be proportional to the square root of the distance from the leading edge of the plate when measured along the streamline of the main-stream flow. The deflection of the boundary-layer flow at the plate surface</p> <p>Copies obtainable from NACA, Washington (over)</p>	<p>NACA TN 2658 National Advisory Committee for Aeronautics. LAMINAR BOUNDARY LAYER OVER FLAT PLATE IN A FLOW HAVING CIRCULAR STREAMLINES. Artur Mager and Arthur G. Hansen. March 1952. 28p. diagrs., tab. (NACA TN 2658)</p> <p>The laminar-boundary-layer development over a semi-infinite flat plate placed in a flow with concentric circular streamlines was investigated with the limitation of small total turning of the main-stream flow. The shape of the velocity profiles in the direction of the main-stream flow and perpendicular to it was analytically determined for an incompressible flow and a compressible flow with Prandtl number equal to 1. The boundary-layer thickness was shown to be proportional to the square root of the distance from the leading edge of the plate when measured along the streamline of the main-stream flow. The deflection of the boundary-layer flow at the plate surface</p> <p>Copies obtainable from NACA, Washington (over)</p>	<p>1. Flow, Viscous (1.1.3) 2. Flow, Laminar (1.1.3.1) 3. Boundary-Layer Characteristics - Internal Aerodynamics (1.4.7.1)</p> <p>I. Mager, Artur II. Hansen, Arthur G. III. NACA TN 2658</p> <p style="text-align: center;"></p>	<p>1. Flow, Viscous (1.1.3) 2. Flow, Laminar (1.1.3.1) 3. Boundary-Layer Characteristics - Internal Aerodynamics (1.4.7.1)</p> <p>I. Mager, Artur II. Hansen, Arthur G. III. NACA TN 2658</p> <p style="text-align: center;"></p>

NACA TN 2658

face from the direction of a circular streamline in the main flow was shown to vary directly with the turning. With increase in the Mach number of the main-stream flow, both the boundary-layer thickness and the deflection increased.

Copies obtainable from NACA, Washington



NACA TN 2658

face from the direction of a circular streamline in the main flow was shown to vary directly with the turning. With increase in the Mach number of the main-stream flow, both the boundary-layer thickness and the deflection increased.

Copies obtainable from NACA, Washington



NACA TN 2658

face from the direction of a circular streamline in the main flow was shown to vary directly with the turning. With increase in the Mach number of the main-stream flow, both the boundary-layer thickness and the deflection increased.

Copies obtainable from NACA, Washington



NACA TN 2658

face from the direction of a circular streamline in the main flow was shown to vary directly with the turning. With increase in the Mach number of the main-stream flow, both the boundary-layer thickness and the deflection increased.

Copies obtainable from NACA, Washington

